Proceedings of the 21st International Conference on Automation & Computing, University of Strathclyde, Glasgow, UK, 11-12 September 2015

Diagnosis of Combination Faults in a Planetary Gearbox using a Modulation Signal Bispectrum based Sideband Estimator

Xiange Tian, Gaballa M. Abdallaa, Ibrahim Rehab, Fengshou Gu and Andrew D. Ball
Centre for Efficiency and Performance Engineering
University of Huddersfield
Huddersfield, UK

Fengshou Gu, Tie Wang
School of Mechanical Engineering
Taiyuan University of Technology
Shanxi, China

***Abstract*—This paper presents a novel method for diagnosing combination faults in planetary gearboxes. Vibration signals measured on the gearbox housing exhibit complicated characteristics because of multiple modulations of concurrent excitation sources, signal paths and noise. To separate these modulations accurately, a modulation signal bispectrum based sideband estimator (MSB-SE) developed recently is used to achieve a sparse representation for the complicated signal contents, which allows effective enhancement of various sidebands for accurate diagnostic information. Applying the proposed method to diagnose an industrial planetary gearbox which coexists both bearing faults and gear faults shows that the different severities of the faults can be separated reliably under different load conditions, confirming the superior performance of this MSB-SE based diagnosis scheme.**

Keywords-Planetary gearbox, Ball bearing, Modulation signal bispectrum, Combination fault diagnosis, Vibration signal.

I. INTRODUCTION

Planetary or epicyclic gearboxes are widely used for the power transmission of important machines such as helicopters, wind turbines, automobiles, aircraft engines and marine vehicles due to their large transmission ratios and strong load-bearing capacity. Gears and bearings are the critical mechanical components in planetary gearboxes. Early fault detection and diagnosis are significant to present any failures of either of these components which can lead to the failure of the entire system. Therefore, many advanced techniques have been investigated to analyze the vibration signals from planetary gearboxes for more accurate diagnosis.

Sawalhi et al. [1] proposed a method based on time synchronous averaging (TSA). Firstly, it isolates and then removes the deterministic components corresponding to each gear in the system by synchronous averaging, leaving a residual stochastic signal which should be dominated by bearing faults in some frequency bands. Then, the residual signal is applied to cepstrum pre-whitening for bearing fault detection. Vishwash et al. [2] used multi-scale slope feature extraction technique based on wavelet multi-resolution analysis, discrete wavelet transform (DWT) and wavelet packet transform (WPT), for fault diagnosis of gear and bearing. For planetary bearing fault diagnosis, Bonnardot and Randall et al. [3] presented an enhanced unsupervised noise cancellation that uses an unsupervised order tracking algorithm to perform noise cancellation in the angular domain. To extract fault features of the rolling element bearing from the masking faulty gearbox signals, Tian et al. [4] explored a method based on WPT, Pearson correlation coefficient and envelope analysis. Elasha et al. [5] developed a method for defective bearings in a planetary gearbox by applying an adaptive filter, spectral kurtosis and envelope analysis to both AE and vibration signals. These efforts in improving data quality have shown different degrees of success in diagnosing fault types and severities.

However, these significant progresses in analyzing the vibration signals are made based on single type of fault cases largely and less attention is paid to multiple faults occurring concurrently which are becoming more significant as the structures of rotating machinery become of larger scale, of higher speed, and more complicated[6]. In addition, these studies usually focused more on noise reduction but with limited efforts on the utilization of multiple modulation characteristics in extracting the diagnostic information.

To fill these gaps, this paper presents a new method for combination fault detection of gear and bearing based on MSB-SE analysis of vibration signals, which has been demonstrated to be particular effective in highlighting sidebands and hence diagnosing faults on gears only [7]. The following content is organized as: Section 2 outlines the theoretical basis of the combination fault diagnosis based on the modulations between different vibration sources. Section 3 describes the experimental setups for validating the proposed method. Then, section 4 presents the diagnostic results and discussion. Finally, section 5 is the conclusion.

II. THEORETICAL BACKGROUND FOR DIAGNOSING THE COMBINATION FAULTS

A. Planetary gearbox vibration characteristics

A planetary gearbox is composed of a ring gear, a sun gear and multiple planet gears. Usually, the ring gear is stationary, a sun gear rotates around a fixed center, and planet gears not only spin around their own centers but also revolve around the center of the sun gear. The planet gears mesh simultaneously with both the sun gear and the ring gear. Due to these complicated gear motions, the

vibration signals generated by planetary gearboxes are more complicated than those by fixed shaft gearboxes. In addition, the planet phasing relationship, which is dependent on the number of planets, planet position angles, and the number of teeth of each gear, also adds complexity to vibration signals. In this section, the planetary gearbox vibration signal models will be introduced. The gear damage could produce the amplitude modulation and frequency modulation (AMFM) effects to the gear meshing vibration at corresponding fault characteristic frequencies [8].

Based on the theoretical analysis in [7], in steady working condition such as constant running load and speed, the vibration perceived by a sensor on the stationary ring can be represented with mutual modulations of both AM and FM phenomena. For a local fault, such as the crack and pitting on one of the tooth of sun gear, the signal model for the 1st sinusoidal component can be expressed as:

$$f(t) = [1-\cos(2\pi f_{rs} t)][1-\cos(2\pi f_{rc} t)][1+A\cos(2\pi f_{sf} t+\phi)] \times \cos[2\pi f_m t + B\sin(2\pi f_{sf} t+\varphi)+\theta] \quad (1)$$

on the planet gear

$$f(t) = [1-\cos(2\pi f_{rc} t)][1-\cos(2\pi f_{rc} t)][1+A\cos(2\pi f_{pf} t+\phi)] \times \cos[2\pi f_m t + B\sin(2\pi f_{pf} t+\varphi)+\theta] \quad (2)$$

and on the ring gear

$$f(t) = [1+A\cos(2\pi f_{rf} t+\phi)][1-\cos(2\pi f_{rc} t)] \times \cos[2\pi f_m t + B\sin(2\pi f_{rf} t+\varphi)+\theta] \quad (3)$$

where f_{sf} , f_{pf} and f_{rf} is the fault characteristic frequency of the sun gear, planet gear and or ring gear respectively. f_{rc} and f_{rs} is the rotating frequency of the carrier and sun gear. f_m is the gear meshing frequency. θ , ϕ and φ are the initial phases of AM and FM respectively.

Therefore, consider the AMFM effects with the high orders of fault gear characteristic frequency nf_{xf} as the modulating frequency and with the higher orders of meshing frequency kf_m as the signal carrier frequency and f_{rx} as the corresponding component rotating frequency, the vibration spectral peaks will appear at the frequency locations of $kf_m \pm nf_{xf} \pm f_{rc}$ and $kf_m \pm f_{rx} \pm nf_{xf} \pm f_{rc}$ $(k, n = 1,2,3\cdots)$ in the Fourier spectrum. From the analysis of vibration spectra, we can detect and locate the gear fault by monitoring the presence of magnitude increase of spectral peaks at the above mentioned frequency locations.

B. *Characteristic Frequencies for Planetary Gear Fault Detection*

According to reference [7], the rotation frequency of carrier can be calculated as

$$f_{rc} = \frac{Z_s}{Z_r + Z_s} f_{rs} \quad (4)$$

the planet gear frequency as

$$f_{rp} = \frac{(Z_p - Z_r)Z_s}{(Z_r + Z_s)Z_p} f_{rs} \quad (5)$$

and the meshing frequency as

$$f_m = (f_{rs} - f_{rc})Z_s = \frac{Z_r Z_s}{Z_r + Z_s} f_{rs} = Z_r f_{rc}, \quad (6)$$

where f_{rs} is the sun gear rotating speed; Z_r , Z_p and Z_s denote the number of teeth for the ring, planet and sun gear respectively.

As shown in many previous studies, detection and diagnosis can be carried out by examining the changes of characteristic frequencies around mesh frequency f_m and its harmonics. Considering that there are K number of planetary gears moving with the carrier, characteristic frequencies around meshing frequency can be calculated [9][10] for different local faults occurring on the sun gear

$$f_{sf} = \frac{f_m}{Z_s} = K(f_{rs} - f_{rc}) \quad (7)$$

on the planet gear

$$f_{pf} = 2\frac{f_m}{Z_p} = 2(f_{rp} + f_{rc}) \quad (8)$$

and on the ring gear

$$f_{rf} = \frac{f_m}{Z_r} = K f_{rc}. \quad (9)$$

However, as shown in [10][11] only some of these expected sidebands will be apparent in the vibration spectrum when a planetary gearbox has faults due to the effects of constructive superposition of the vibration waves from the three gear sets, whereas other sidebands are hard to be seen because of the destructive effect of the superposition, and hence the latter have been largely neglected by previous studies when developing methods for fault diagnosis.

C. *Characteristic Frequencies for Bearing Fault Detection*

A ball bearing consists of an inner race, an outer race, several balls and a cage, which holds the balls in a given relative position. Race surface fatigue results in the appearance of spalls on the inner race, outer race or balls. If one of the races has a spall, it will almost periodically impact with the balls. The fault signature is represented by successive impulses with a repetition rate depending on the faulty component, geometric dimensions and the rotational speed. The period between impacts is different for all the listed elements and depends on the geometry of the bearing, the rotational speed and the load angle. For a fixed outer race bearing, the theoretical characteristic fault frequencies can be calculated using (10)-(13), and a derivation of these equations is presented in [12].

Fundamental cage frequency:

$$F_c = \frac{1}{2} F_s \left(1 - \frac{D_b}{D_c}\cos\alpha\right) \quad (10)$$

Outer race defect frequency:

$$F_o = \frac{N_b}{2} F_s (1 - \frac{D_b}{D_c} \cos \alpha) \quad (11)$$

Inner race defect frequency:

$$F_i = \frac{N_b}{2} F_s (1 + \frac{D_b}{D_c} \cos \alpha) \quad (12)$$

Ball defect frequency:

$$F_b = \frac{D_c F_s}{2 D_b} (1 - \frac{D_b^2}{D_c^2} \cos^2 \alpha) \quad (13)$$

where D_c is pitch circle diameter, D_b is ball diameter, α is contact angle, N_b is number of ball and F_s is shaft rotational frequency.

While the sensor is mounted on the gearbox housing, which is connected to or fastened to the ring gear directly, the bearing damage induced vibration has two main paths to go from its source to the senor through solid mechanical components and their contacts. Through the first path, the vibration signal propagates from its origin to the gearbox casing, and then reaches the sensor. Whereas through the second path, the vibration signal follows a longer path, from its origin to the shaft firstly, then from the shaft go through the sun gear, planet gear and ring gear, after that from the ring gear to the gearbox casing, and finally to the sensor. Therefore, the vibration signal will be amplitude modulated by both sun gear rotating frequency and carrier rotating frequency as shown in (14).

$$\begin{aligned} f(t) = &[1 - \cos(2\pi f_{rs} t)] \cos[2\pi f_{bx} t + \alpha] \\ &+ [1 - \cos(2\pi f_{rc} t)] \cos[2\pi f_{bx} t + \alpha] \end{aligned} \quad (14)$$

where f_{bx} is the characteristic frequency of bearing.

In practice there is always slight slippage, especially when a bearing is under dynamic loads and with severe wear. Therefore, these frequencies may have a slight difference from calculated ones above. In this paper, the experiment bearing is located on the output shaft of planetary gearbox which is closed to sun gear. It is a 6008ZZ deep groove ball bearing and its geometric dimensions that needed for fault frequency calculation are listed in Table I.

TABLE I. SPECIFICATION OF EXPERIMENT BALL BEARING

Parameter	Measurement
Pitch Diameter	54 mm
Ball Diameter	7.398 mm
Ball Number	12
Contact Angle	0

D. Modulation Signal Bispectrum

For a vibration signal $x(t)$ with corresponding Fourier Transform (FT) $X(f)$, the MSB-SE can be obtained by

$$B_{MS}^{SE}(f_c, f_s) = E\left[\frac{X(f_c + f_s) X(f_c - f_s) X^*(f_c) X^*(f_c)}{|X(f_c)|^2}\right] \quad (15)$$

where the product between the upper sideband $X(f_c + f_s)$, the lower sideband $X(f_c - f_s)$ and the normalized carrier component $X^*(f_c)X^*(f_c)/|X(f_c)|^2$ allows the sideband effect to be combined and quantified without the effect of the carrier amplitude. Moreover, because of the average operation, denoted by the expectation operator $E[\ ]$ in (15), the sideband products which associate with a constant phase value can be enhanced, while the noise and interfering components with random phases are suppressed effectively. This MSB based approach has been shown to yield outstanding performance in characterizing the small modulating components of motor current signals for diagnosing different electrical and mechanical faults under different load conditions [13][14][15]. Therefore, it is also evaluated in this study to extract the residual sidebands of vibration signal for the purpose of gear and bearing fault diagnosis.

III. EXPERIMENTAL SETUPS

To verify the effectiveness of MSB-SE based diagnosis, vibration signals were acquired from an in-house planetary gearbox test system. The maximum torque of planetary gearbox is 670 Nm, the maximum input speed is 2800 rpm and maximum output speed is 388 rpm. The schematic in Fig. 1 shows the position of the accelerometer that mounted on the outer surface of the ring gear and the position of experiment studied bearing.

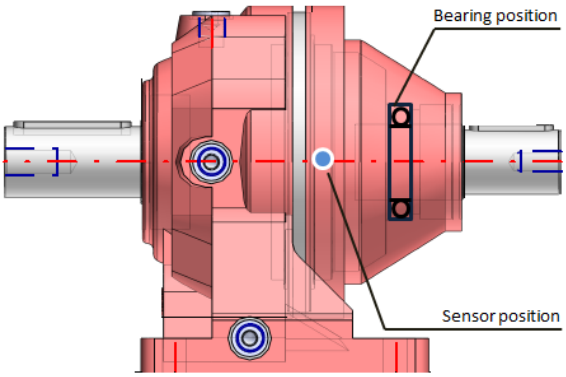

Figure 1. Schemetic for a planetary gearbox

In the experiment, the planetary gearbox operates at 80% of its full speed under 5 load conditions (0%, 25%, 50%, 75% and 90% of the full load). The load setting allows fault diagnoses to be examined with variable load operations which are the cases for many applications such as wind turbine, helicopters etc. The vibration is measured by a general purpose accelerometer with a sensitivity of 31.9 mv/(ms^{-2}) and frequency response ranges from 1Hz to 10kHz. All the data were logged simultaneously by a multiple-channel, high-speed data acquisition system with 100 kHz sampling rate and 16-bit resolution.

Figure 2. Tooth defects simulated on the sun gear and two kinds of inner race defect on deep groove ball bearing

Three cases of test were carried out to examine the combination faults. The first one is health case, in which

there is no defect on either the gear or bearing. The second one is for the combination fault of small bearing inner race defect and sun gear tooth defect. The third one is for the combination fault of large bearing inner race defect and sun gear tooth defect. For the convenience of discussion, these three cases are denoted as Healthy, CbFault1 and CbFault2, respectively. Fig. 2 shows the defects on sun gear and bearing inner races.

IV. Diagnostic Results and Discussion

A. Spectrum Features of Vibration Signals

Fig. 3 shows the typical spectra for the three cases under the same load. They exhibit complicated patterns and high density of spectral component, which needs careful examination to find the components of interest. Three distinctive peaks close to the first three mesh frequencies appear at $f_m + f_{rc}$, $2f_m - f_{rc}$ and $3f_m$ respectively, which agrees with the model prediction and that of previous studies[10][11][16]. However, there are also many distinctive peaks between two mesh frequencies. For example, the components at $2f_m - 6f_{sf} - 1f_{rc}$, $2f_m + 7f_{sf}$ etc. should not appear for a healthy planetary gearbox. The presence of these peaks may due to the gearbox manufacturing and installation errors. The green dash lines show the bearing inner race fault frequency and it harmonics. It is obvious that their amplitudes are quite small compared with the other components. This makes it difficult for reliable bearing fault diagnosis. Therefore, the modulation effects between the bearing fault frequency and other characteristic frequencies such as f_{rs} and f_{rc} are used for bearing fault diagnosis.

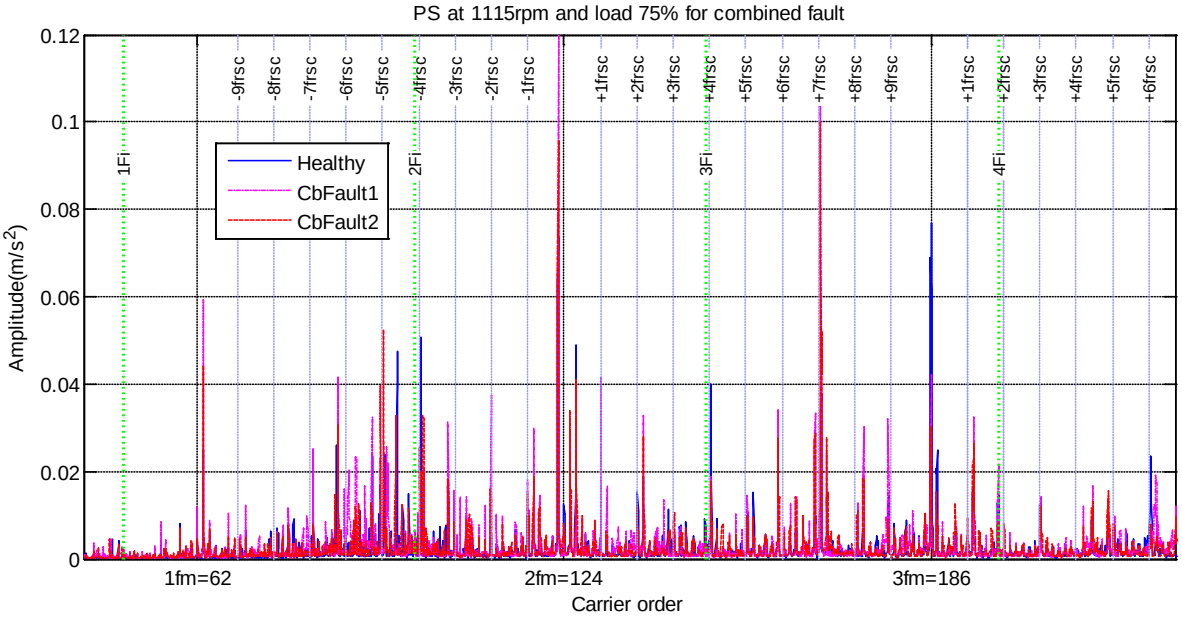

Figure 3. Spectra for different fault cases of the gearbox at 1115 rpm and 75% load.

B. MSB Features of Vibration Signals

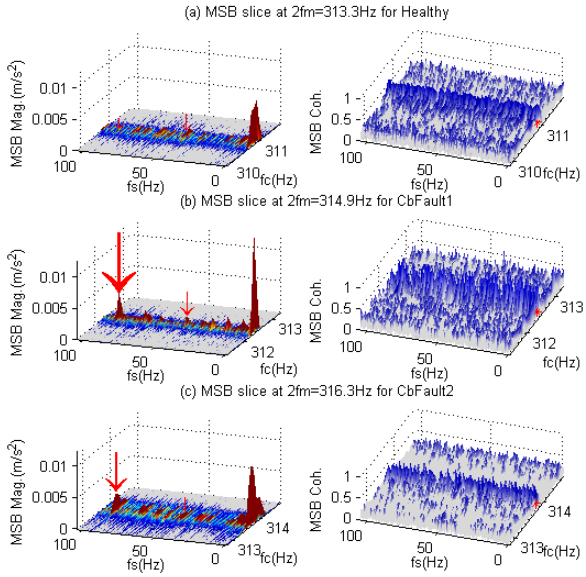

Figure 4. MSB results for different cases of the tests under 75% load.

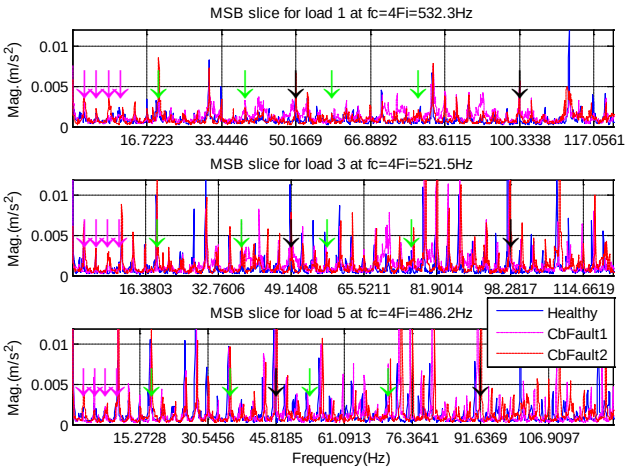

Figure 5. MSB slice for different cases at $f_c = 4F_i$.

Fig. 4 shows a typical MSB result for the three cases of test under 75% load. To show a clear change of the residual sidebands around mesh frequency $2f_m = 313Hz$, MSB and its corresponding coherence results are

presented in the bifrequency domain in the region of $f_c \le 2f_m \pm 1 = 313 \pm 1Hz$ and $f_s < 100Hz$ to include the sidebands up to $6f_{sf}$.

Fig. 5 illustrates the MSB slices at $f_c = 4F_i$ for bearing fault detection. The pink, green and black arrows show the sideband at f_{rc}, f_{rs} and f_{sf} respectively. They show differences between baseline, small bearing inner race defect and large bearing inner race defect cases.

C. Diagnosis of Sun Gear Fault

The diagnostic results for the sun gear are presented in Fig. 6. From the results of residual sidebands obtained from the MSB slice at $2f_m - f_{rc}$, it can be seen that the amplitudes at f_{sf} show a good increasing trend with loads, which agrees with the load characteristics of gear transmissions. Moreover, these amplitudes show clear incremental differences between three tested cases under high load. Therefore, they can be used for obtaining fault diagnosis reliably.

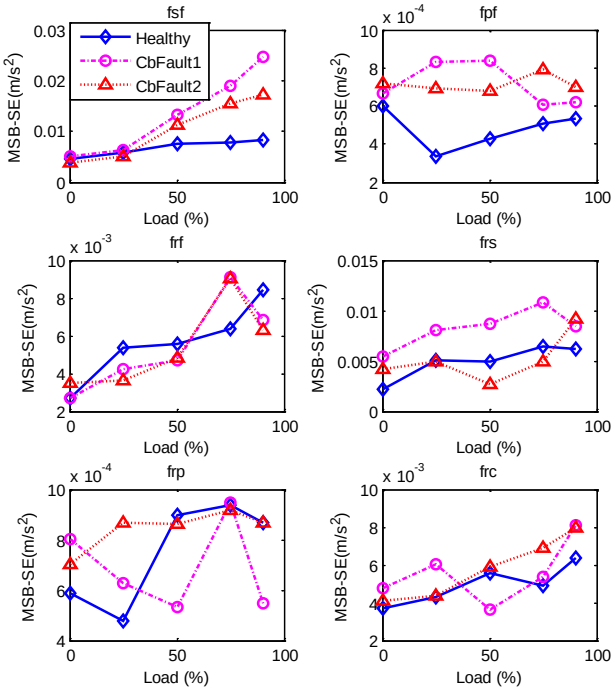

Figure 6. MSB-SE diagnosis results of the sun gear faults using the slice at $f_c = 2f_m - f_{rc}$.

The corresponding MSB coherence results are printed in Fig. 7, which can be used to assure the reliably of MSB-SE results. From the figure it can be seen that the MSB coherence is low at f_{pf} and f_{rp}, which indicates that there is no significant modulation phenomena at these two sidebands. It means there is no fault on planetary gear and ring gear. Meanwhile, the amplitude changes for other characteristic frequencies are also provided to assure the diagnostic results. These changes exhibit high fluctuations with the fault progression and the load increases, which is not consistent with the gear dynamic characteristics in that the fault usually causes higher vibrations and also increases with load. Therefore, they cannot be used to indicate the corresponding faults but just caused by refitting errors.

Therefore, the fault location can be identified by checking the feature that the increase in residual sidebands occurs over several different loads simultaneously.

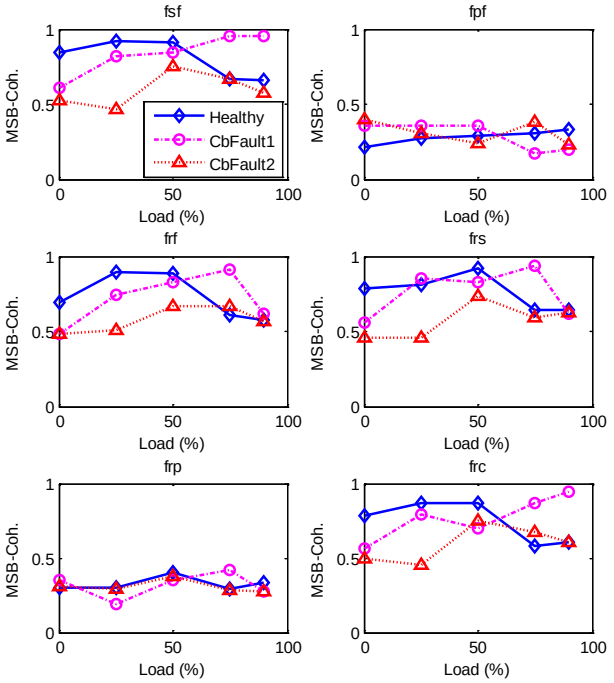

Figure 7. MSB coherence results of the sun gear faults using the slice at $f_c = 2f_m - f_{rc}$.

D. Diagnosis of Bearing Fault

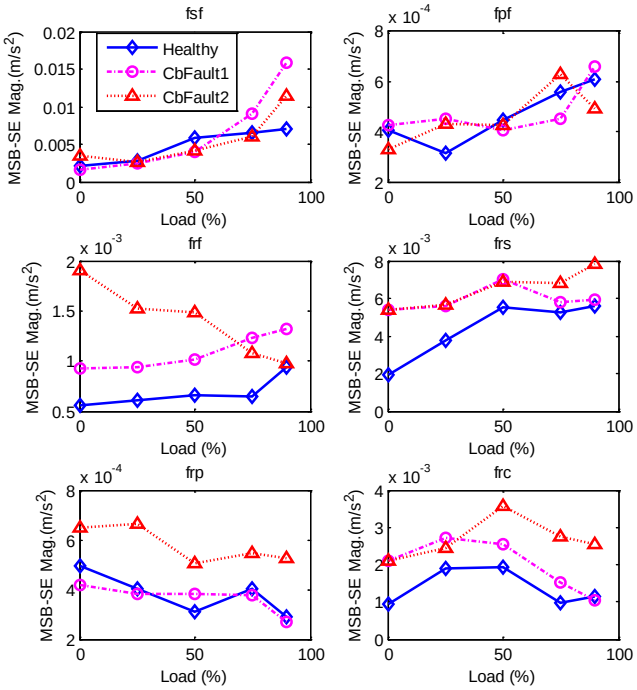

Figure 8. Averaged MSB-SE diagnosis results of the small bearing faults using the slices at $f_c = F_i$ and $f_c = 4F_i$.

From the spectrum in Fig. 3 it can be seen that the characteristic frequency of bearing fault and its harmonics may be interfered by the complex gearbox frequency components. Some harmonic amplitudes may be greatly reduced which is not conductive to bearing fault diagnosis. Therefore, only the harmonics with high coherence values will be selected for bearing fault diagnosis.

In this paper, MSB slices at $f_c = F_i$ and $f_c = 4F_i$ are selected for fault detection because of their high coherences. The averaged MSB-SE and MSB coherence results are presented in Fig. 8 and Fig. 9, respectively. Compared with other feature components, the features at f_{rs} and f_{rc} have higher coherence amplitudes, showing high potential of modulation effects between the fault characteristic frequencies and their closer interacting components. This thus confirms the presence of the inner race fault on the bearing. However, they can only separate small inner race fault from the larger under the high load conditions where the modulations are stronger.

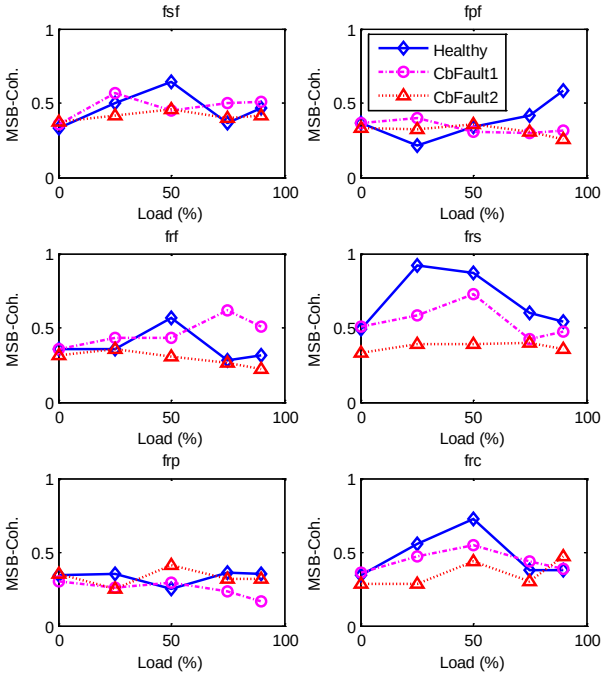

Figure 9. Averaged MSB coherence results of the small bearing faults using the slice at $f_c = F_i$ and $f_c = 4F_i$.

V. CONCLUSIONS

In this paper, a combination fault diagnosis method based on MSB-SE is developed for the monitoring faults on both bearing and gear in a planetary gearbox. MSB analysis is effective in suppressing random noise and decomposing the nonlinear modulation components in the measure vibration signals. Thus, the sideband amplitudes extracted by MSB-SE at the MSB slices relating to characteristic frequencies have more reliable information on the fault which causes the sidebands.

The method was verified with experimental data from a planetary gearbox with combined gear and bearing faults. The diagnostic results show that not only the types of the combination faults: defects in bearing inner race and tooth breakages of sun gear can be separated but also the severity of the two faults can be estimated successfully under high load conditions.

REFERENCES

[1] N. Sawalhi, R. Randall and D. Forrester, 'Separation and enhancement of gear and bearing signals for the diagnosis of wind turbine transmission systems', *Wind Energy*, vol. 17, no. 5, pp. 729-743, 2013.

[2] B. Vishwash, P. S. Pai, N. S. Sriram, R. Ahmed, H. S. Kumar, and G. S. Vijay, "Multiscale Slope Feature Extraction for Gear and Bearing Fault Diagnosis Using Wavelet Transform," *Procedia Materials Science*, vol. 5, pp. 1650–1659, 2014.

[3] Bonnardot, F., R. B. Randall, J. Antoni, and F. Guillet. "Enhanced unsupervised noise cancellation using angular resampling for planetary bearing fault diagnosis." *International journal of acoustics and vibration*, vol. 9, no. 2, pp. 51-60, 2004.

[4] J. Tian, M. Pecht and C. Li, 'Diagnosis of rolling element bearing fault in bearing-gearbox union system using wavelet packet correlation analysis', Dayton, OH, 2012, pp. 24-26.

[5] E. Faris, M. Greaves and D. Mba, 'Diagnostics of a defective bearing within a planetary gearbox with vibration and acoustic emission', in *The 4th International Conference on Condition Monitoring of Machinery in Non-Stationary Operations (CMMNO 2014)*, Lyon, France, 2014.

[6] Q. Zhang, Q. Hu, G. Sun, X. Si and A. Qin, 'Concurrent Fault Diagnosis for Rotating Machinery Based on Vibration Sensors', *International Journal of Distributed Sensor Networks*, vol. 2013, pp. 1-10, 2013.

[7] F. Gu, G. Abdalla, R. Zhang, H. Xu and A. D. Ball, 'A Novel Method for the Fault Diagnosis of a Planetary Gearbox based on Residual Sidebands from Modulation Signal Bispectrum Analysis', in *Comadem 2014*, Brisbane, Australia, 2014.

[8] Z. Feng and M. Zuo, 'Vibration signal models for fault diagnosis of planetary gearboxes', *Journal of Sound and Vibration*, vol. 331, no. 22, pp. 4919-4939, 2012.

[9] Y. Lei, J. Lin, M. Zuo and Z. He, 'Condition monitoring and fault diagnosis of planetary gearboxes: A review', *Measurement*, vol. 48, pp. 292-305, 2014.

[10] L. Hong, J. Dhupia and S. Sheng, 'An explanation of frequency features enabling detection of faults in equally spaced planetary gearbox', *Mechanism and Machine Theory*, vol. 73, pp. 169-183, 2014.

[11] M. Inalpolat and A. Kahraman, 'A theoretical and experimental investigation of modulation sidebands of planetary gear sets', *Journal of Sound and Vibration*, vol. 323, no. 3-5, pp. 677-696, 2009.

[12] T. Barszcz and N. Sawalhi, 'Fault Detection Enhancement in Rolling Element Bearings Using the Minimum Entropy Deconvolution', *Archives of Acoustics*, vol. 37, no. 2, pp.131-141, 2012.

[13] A. Alwodai, F. Gu, A. D. Ball, 'A comparison of different techniques for induction motor rotor fault diagnosis'. *Journal of Physics: Conference Series* 364, 1742-6596, 2012.

[14] Z. Chen, T. Wang, F. Gu, H. Mansaf, A. D. Ball. 'Gear Transmission Fault Diagnosis Based on the Bispectrum Analysis of Induction Motor Current Signatures', *Journal of Mechanical Engineering*, vol. 48, no. 21, pp. 84-90, 2012.

[15] F. Gu, T. Wang, A. Alwodai, X. Tian, Y. Shao and A. D. Ball, 'A new method of accurate broken rotor bar diagnosis based on modulation signal bispectrum analysis of motor current signals', *Mechanical Systems and Signal Processing*, vol. 50-51, pp. 400-413, 2015.

[16] P. McFadden and J. Smith, 'An Explanation for the Asymmetry of the Modulation Sidebands about the Tooth Meshing Frequency in Epicyclic Gear Vibration', *Proceedings of the Institution of Mechanical Engineers, Part C: Journal of Mechanical Engineering Science*, vol. 199, no. 1, pp. 65-70, 1985.